"Seen and approved"

Director General

"ALFA" CJSC

V.A. Osipov

"....."..... 2001

/Seal/

AIRES

New Medical Technologies Foundation

Saint Petersburg

"Seen and approved"

Director General of the State Unitary Enterprise Russian Research Center

"S. I. Vavilov State Optical Institute"

member of the Russian Academy of Sciences

G.T. Petrovskiy

/Seal/

State Unitary Enterprise Russian Research Center /illegible/

"S. I. Vavilov State Optical Institute"

S.I. Vavilov SOI

REPORT № 2

Theoretical and experimental studies of diffraction and polaroid properties of optical transparencies and matrices by AIRES NMTF with a fractal pattern on photomasks

Research work code – "Photomask"

"Approved"

Director of "State Optical Institute TKS-OPTIKA", OJSC

Candidate of Technical Sciences

/signature/ Ye.A. Iozep

Head of the Fundamental Research Laboratory of Fractal Optics: **G.S. Melnikov**

Saint Petersburg

2001

2.4.1. Mathematical model of designing graphically synthesized Aires holograms.

Methods of space-time filtration in optics were proposed over 100 years ago by Ernst Abbe.[1] Contemporary studies of complex spatial filtration using binary masks [2] lead to a whole new scientific field of computer-generated holograms (CGH, so far over 200 research papers have been written in the new area). A number of scientific studies deal with methods of creating raster axes using computer holograms (multiple Hough transform slices, HT CGH) [3] .

In all contemporary works, the mentioned phenomena are explained through complex-valued equations of spatial frequencies written in general terms, and conditions of adequacy are found for points (x,y) in the images generated by the transparencies or diffraction patterns

$$-\frac{q}{2} \le \frac{x}{T} + \frac{\phi(x,y)}{2\pi} + n \le \frac{q}{2} \tag{2.72}$$

where q —is the constant determining the width of the interference fringe

T — is the period of the diffraction grating

$\phi(x,y)$ — is a function of phase variations of the wavefront

n — is an integer

This theoretical approach satisfactorily explains phenomena generated by graphic transparencies with a regular array (matrix) of gratings called diffraction gratings. However, it is applied to spatial periods that hundreds and thousands of times exceed the wavelength of the coherent radiation going through the transparencies.

If the periods of such gratings exceed the wavelength of light radiation, and still generate ordered rasters of beams, these phenomena are customarily qualified as phenomena of diffraction on the edge of dark-field fringes. In truth, there is no reliable mathematical description of these phenomena.

Besides, this theoretical apparatus is not applicable to graphic transparencies with a strictly hierarchical high-density geometric fractal pattern similar to the one shown in Fig. 2.10.

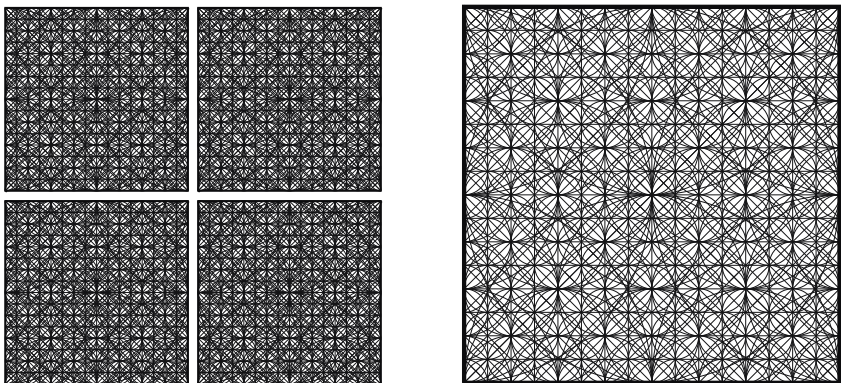

a) A matrix fragment b) The pattern of a matrix element

Fig. 2.10. The matrix of transparencies with a high-density fractal pattern.

However, the transparencies shown in Fig 2.10 create holographic images of raster axes in a broad band of frequencies (Fig. 2.11 a) and are shapers of multiple Hough transform slice–effects (Fig. 2.11 b). The fact that these optical phenomena were formed by the matrix topologies technologically developed and produced as per the terms of reference specifications of AIRES NMTF was experimentally established in operation of transparencies both in conducting and reflecting coherent and non-monochromatic light [43].

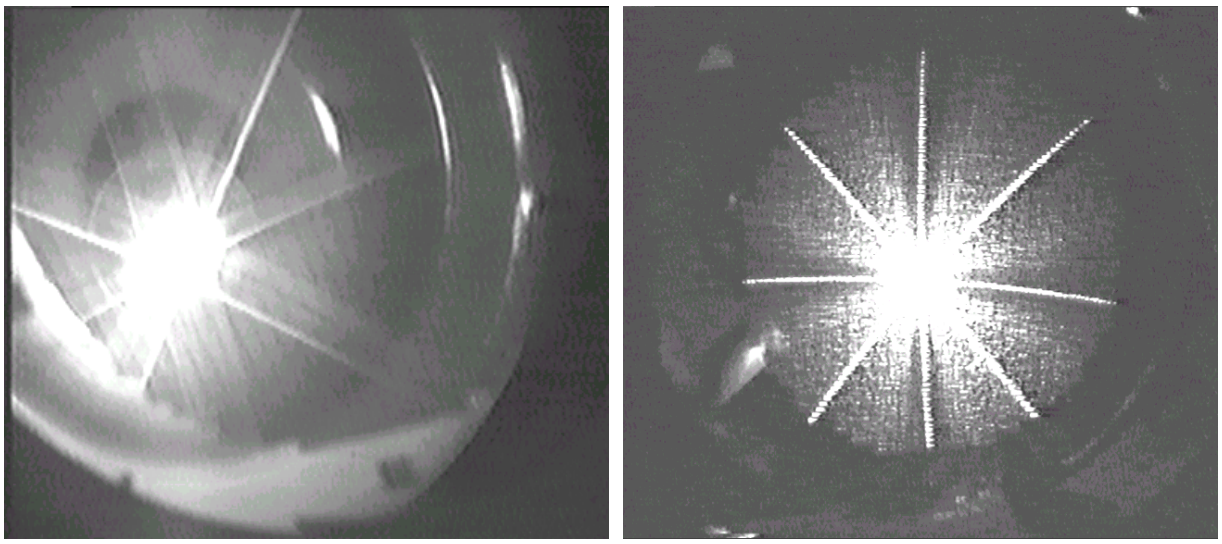

a) b)

Fig. 2.11 Generation of multiple Hough transform slice effects by a transparency matrix

Interference studies also revealed that high-density graphic fractal patterns on transparencies reflecting coherent radiation have optical super power (see Fig. 2.12).

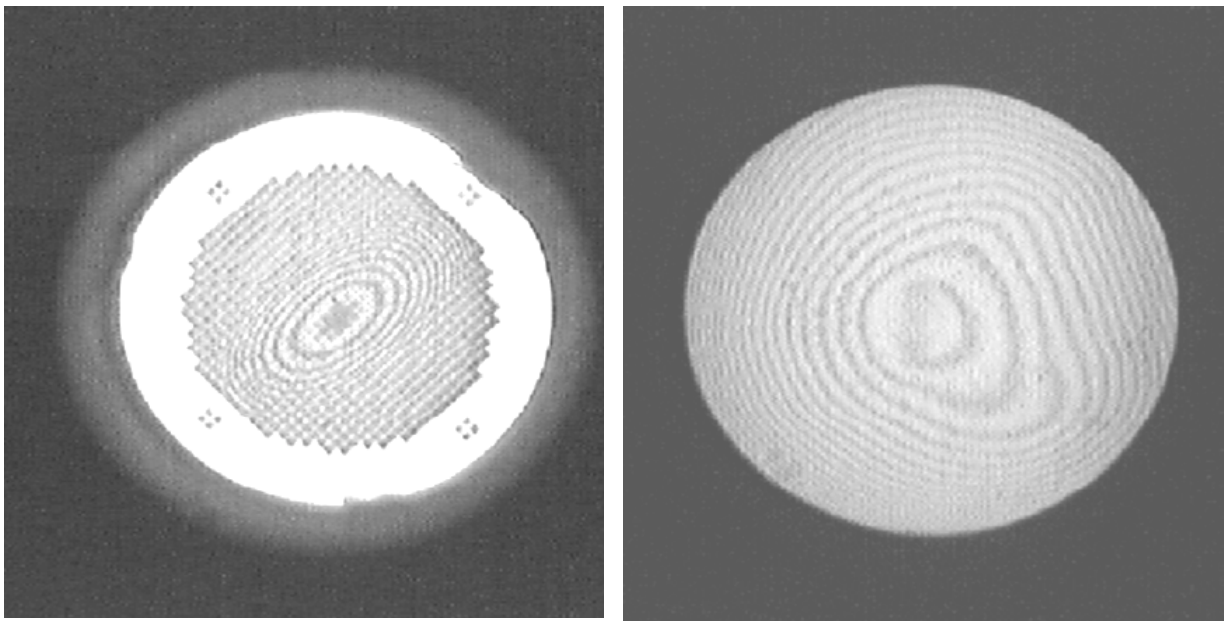

a) From a transparency matrix b) From photomasks

Fig. 2.12. Interference images from transparencies with a high-density fractal pattern working in reflection.

The joint paper [40] based on the experimental studies allows us to argue that most acceptable for describing fixed optical phenomena and a number of detected Fractal optical phenomena [38,39] is the new mathematical model of describing harmonic processes (both spatial and frequency ones) using the methods of the geometric field of spatial frequencies [43].

2.6. Experimental studies of Aires photomasks and transparencies with a phase pattern on glass

2.6.1. A study of geometrical dimensions of matrix elements

There are different methods to measure geometrical dimensions of nano- and subnanodimensional elements that form on the surface of conductive and dielectric substrates. To determine height, width and shape of steps, lines, protrusions (pathways) and grooves (depressions, pits), they used translucent and raster electron beam microscopes; atomic-force, tunneling electron and near-field optical microscopes; light-optical microinterferometers; amplitude- and phase-contrast light microscopes.

At this stage in the study of matrix transparencies it was decided to use the methods of light-optical microinterferometry based on a broad range of structures contained in matrices made by different methods. This simplifies comparative analysis of the structures in question because it is possible to simultaneously observe the magnified image and the change in line height and groove depth.

The layout and operating principle of the interference microscope were once proposed by the outstanding scientist of the Optical Institute, member of the Russian Academy of Sciences V.P. Linnik and applied to study the quality of surface treatment and measure the height of irregularities with the range of 0.03–1 mcm.

The effect of the microscope is based on the phenomenon of light interference. To obtain two wave systems able to interfere, one splits cones of rays outgoing from one point of a light source into two cones. A slanting parallel-sided plate with a semitransparent beam-splitting coating is used as a dividing system. The plate reflects half of the incident light and conducts the other half, thus there occur two wave systems that can interfere. The reference planar wavefront is reflected from a nontransmitting reference mirror, and the object-based wavefront is the light reflected off the specimen in question, carrying information on the geometric structure of the surface, which is encoded in its local change of length of the optical path or phase.

Due to interference of these two wave systems, interference fringes are observed in the focal plane of the ocular. In the points of the field where the path difference is equal to λ, 2λ, 3λ etc., interference produces light fringes, and in the points where the path difference is equal to $\lambda/2$, $3\lambda/2$, $5\lambda/2$ etc. – dark fringes.

Within the field of view of the microinterferometer one can see simultaneously the surface in question and the interference fringes. The interference fringes curve on the surface in question where there are protrusions or depressions. The magnitude of fringe curvature characterizes the size of the surface irregularity and is measured with an eyepiece micrometer.

Microscope magnification during visual examination in a screw eyepiece micrometer is 490 X. The microscope stage can move its positioning in two mutually perpendicular directions (10 mm in each) and rotate at 360 ^{O}. The division value of the fine adjustment crews is 0.005 mm. The microscope ensures examination in regular and monochromatic light. Monochromatic light is produced by placing a green interference light filter in the illuminator.

In white light, the interference fringe pattern appears as follows: in the center there is a white achromatic fringe, on both sides of which there are two black fringes with colored borders, and then 3–4 colored fringes on each side.

Transition from one light (or dark) fringe to another light (or dark) fringe matches the change in the path difference between interfering beams for one wavelength. If the surface in question has a protrusion or depression of λ/2, the interference fringes in this spot will shift by one inter-fringe interval. If the wavelength of light is known, one can find the magnitude of the irregularity in microns. Thus, for example, a 0.275-micron depth of irregularity on the surface will produce a curvature of the fringe within the instrument's field of view for the value of the whole interval between fringes, i.e. "for one fringe." When using light with λ = 0.53 mcm, the smallest irregularity measurable with a microinterferometer, is 0.0265 mcm.

The value of the irregularity is determined in three operations:

1) measuring the value of the interval between fringes,
2) measuring the value of fringe curvature,
3) calculating the height of the irregularity.

When working in white light, the curvature into one interference fringe matches the height of the irregularity on the examined surface, which is 0.275 microns. Then the measured irregularity height t is calculated according to the formula:

$$t = 0.275n(N3 - N4)/ (N1 - N2) , \quad (2.98)$$

where t is the height of the irregularity /mcm/,

N1 is the first count in measuring the interval,
N2 is the second count in measuring the interval,
N3 is the first count in measuring the fringe,
N4 is the second count in measuring the fringe,
n is the number of intervals between fringes.

Sample No. 1. is thin cone-shaped lines (protrusions) generated on the surface of plate glass.

The average height of the pattern lines is 0.5 mcm, the line width at the base is 0.5–0.6 mcm.

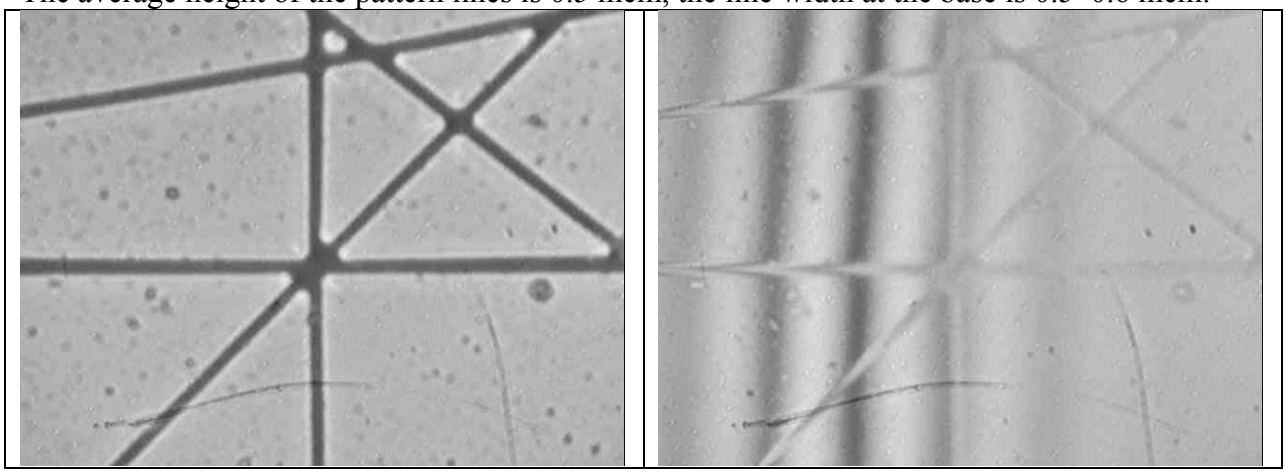

Fig. 2.28 shows a view of the microinterferometer's field of vision in the mode of observation of interference using sample No. 1.

Sample No. 2. appears as thin cone-shaped lines (grooves) generated on the surface of plate glass. The grooves are trapezoid-shaped. The width of the groove on the surface is 15 mcm, on the bottom 7.5 mcm.

The average groove depth is 5 mcm.

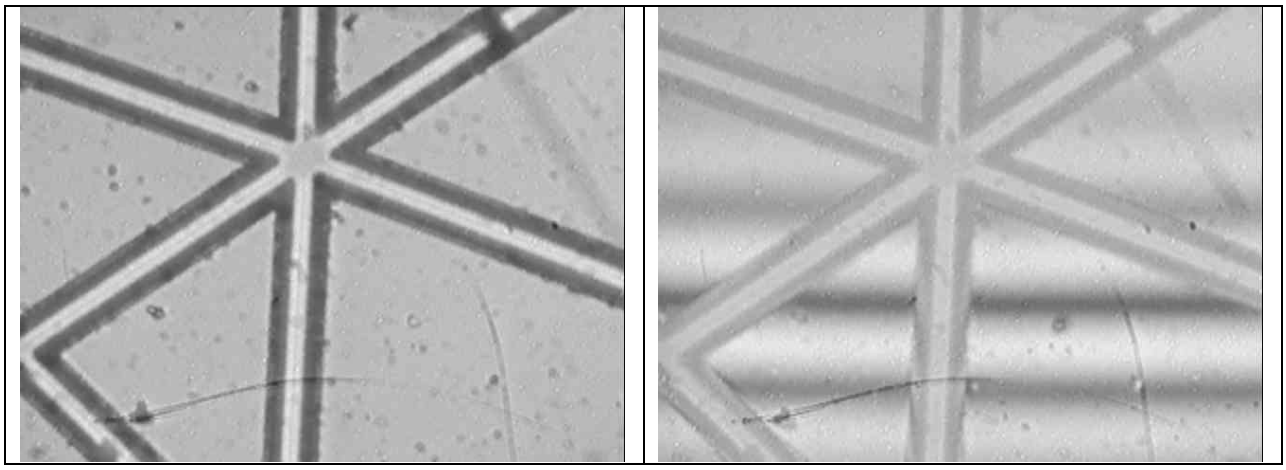

Fig. 2.28 shows a view of the microinterferometer's field of vision in the mode of observation of interference using sample No. 2.

Sample No. 3. It appears as thin cone-shaped lines (protrusions) generated on the surface of plate glass. The average line height is 0.4 mcm. The line width is 0.6…1.2 mcm.

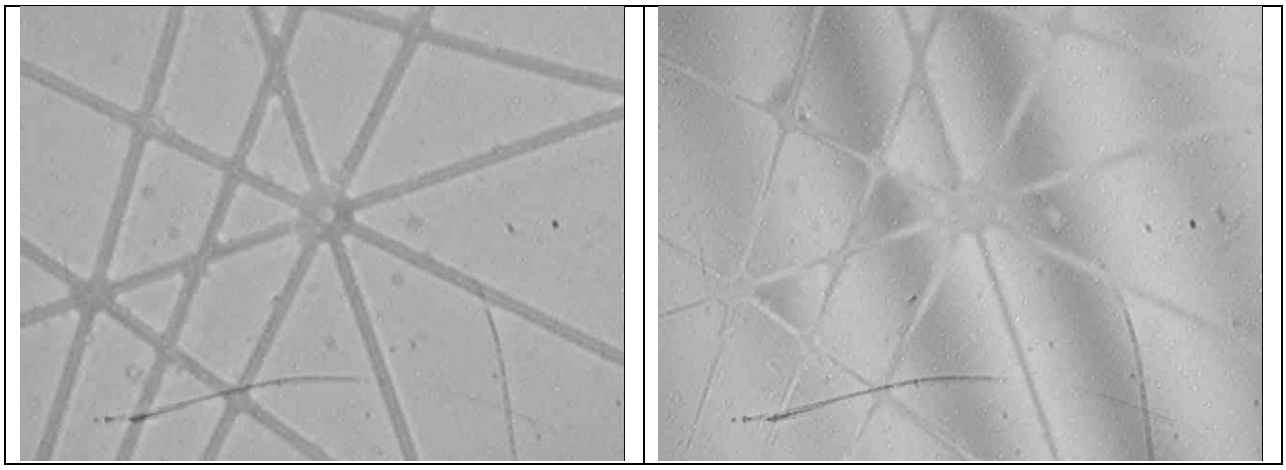

Fig. 2.28 shows a view of the microinterferometer's field of vision in the mode of observation of interference using sample No. 3.

Sample No. 4. It appears as thin cone-shaped lines (grooves) generated on the surface of plate glass. The grooves are trapezoid-shaped. The width of the groove on the surface is 15 mcm, on the bottom 6 mcm. The average depth is 5 mcm.

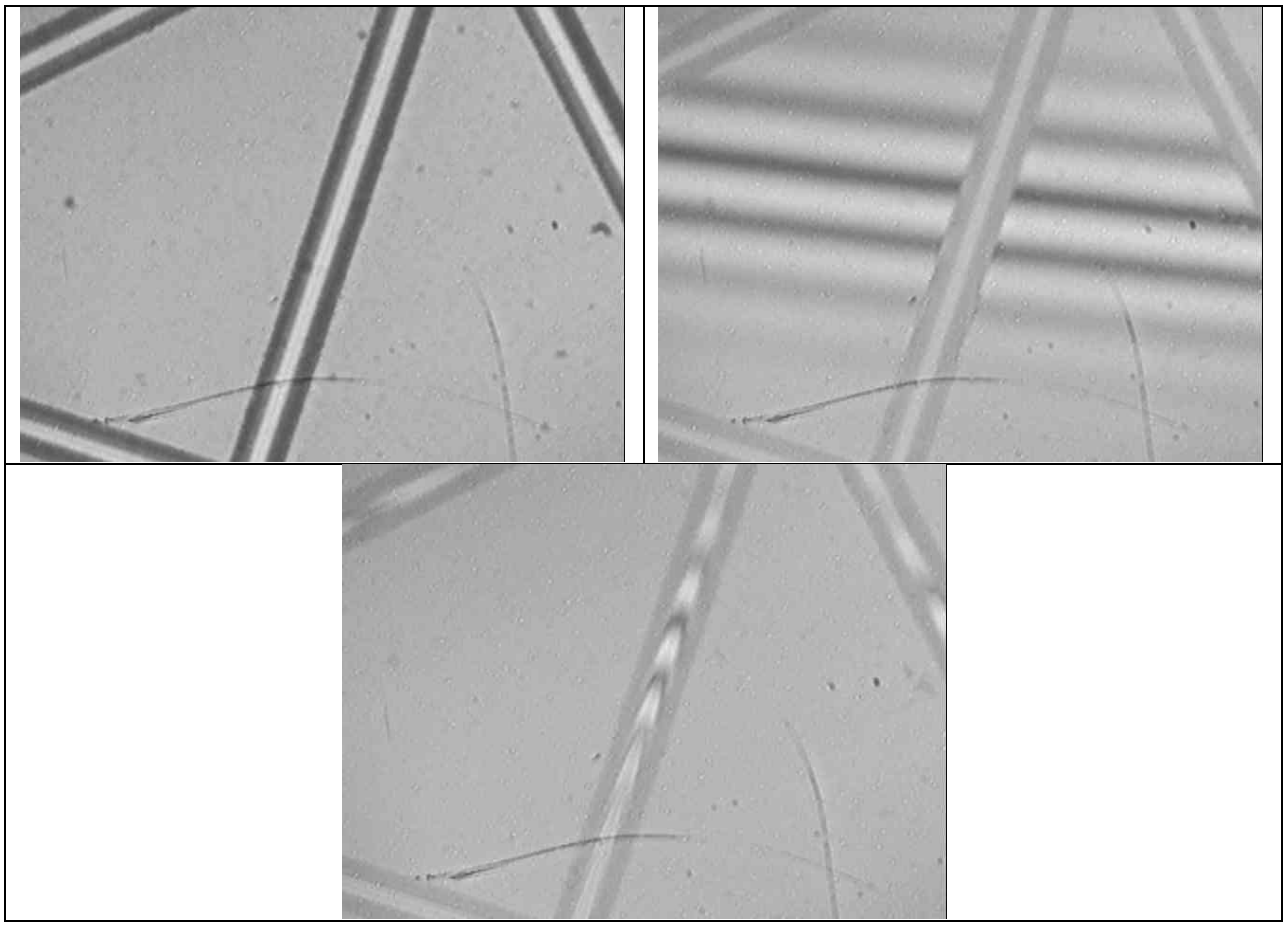

Fig. 2.28 shows a view of the microinterferometer's field of vision in the mode of observation of interference using sample No. 1.

Sample No. 5. appears as a square window in the slightly transparent metal coating on plate glass. In the window there is a matrix pattern (positive) in the form of nontransparent lines. The thickness of the lines in the matrix pattern (the thickness of the metal coating) is approximately 0.05 mcm. Thickness is difficult to measure because light is not reflected by the pathways in the matrix pattern. The linewidth is 4.2 mcm.

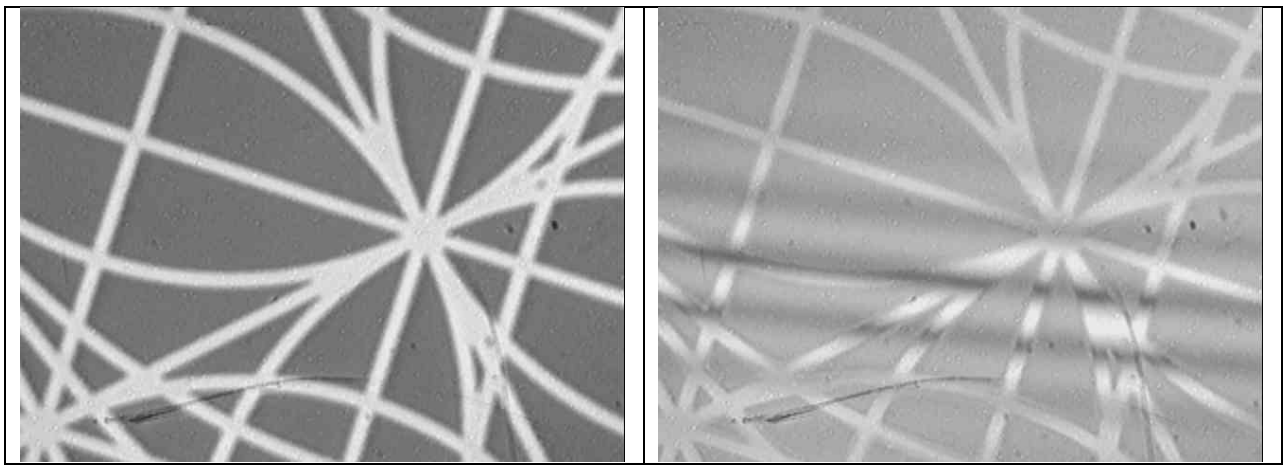

Fig. 2.28 shows a view of the microinterferometer's field of vision in the mode of observation of interference using sample No. 5.

Sample No. 6. appears as a square window in the almost nontransparent metal coating on plate glass. In the window there is a matrix pattern in the form of nontransparent lines (negative).

The thickness of the pattern's metal coating is approximately 0.05 mcm. The layer thickness is difficult to measure because light is not reflected by the lines in the matrix pattern. The linewidth is 3.4 mcm.

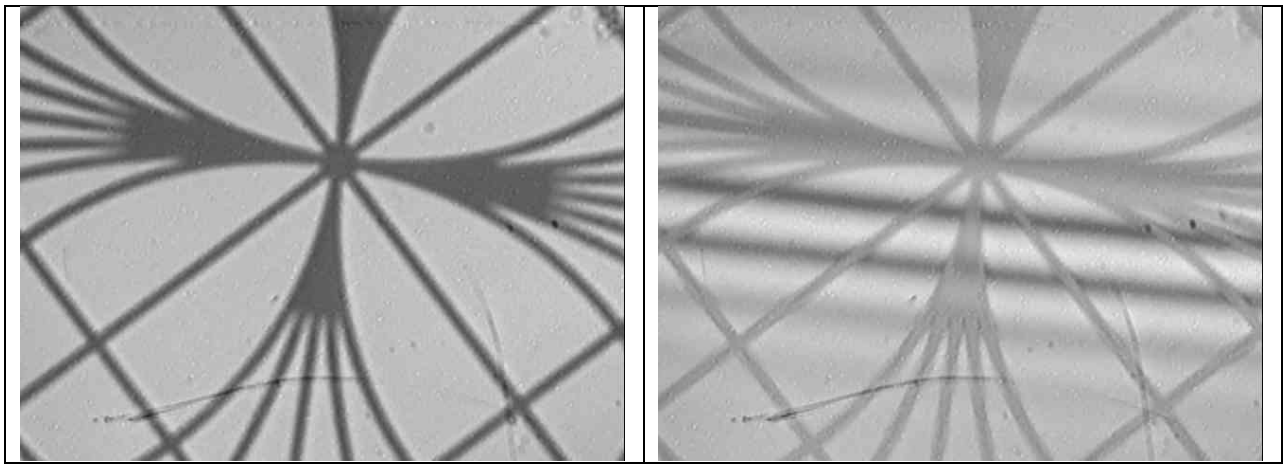

Fig. 2.28 shows a view of the microinterferometer's field of vision in the mode of observation of interference using sample No. 6.

Sample No. 7. appears as a 7 x 7 mm square matrix. The thickness of the line is 0.27 mcm. The linewidth is 0.6–0.9 mcm.

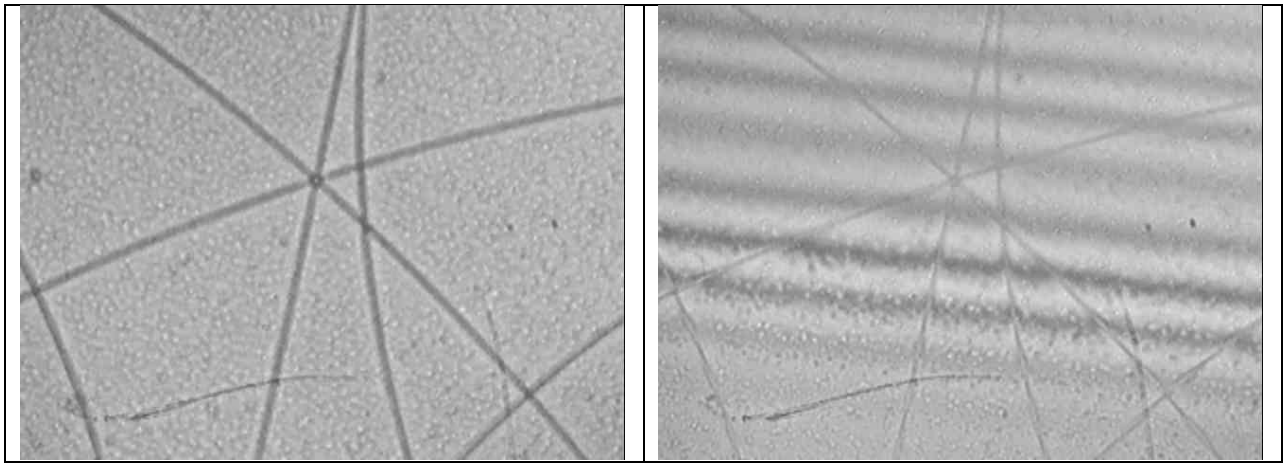

Fig. 2.28 shows a view of the microinterferometer's field of vision in the mode of observation of interference using sample No. 7.

Sample No. 8. appears as a printing copy of a matrix pattern (ferromagnetic layer on an aluminum substrate). The substrate coating is a globular structure with a globule size of 1–20 mcm. Globules have a sharp edge and a dividing line from neighbors.
The linewidth of the pattern is approximately 60 mcm.

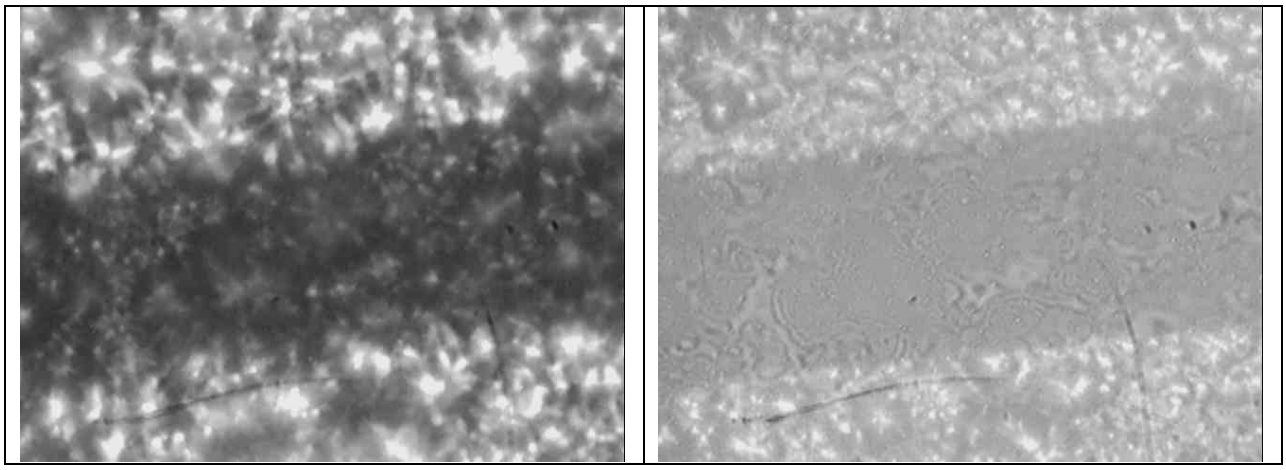

Fig. 2.34 shows a view of the microinterferometer's field of vision in the mode of observation of the image and interference using sample No. 6.

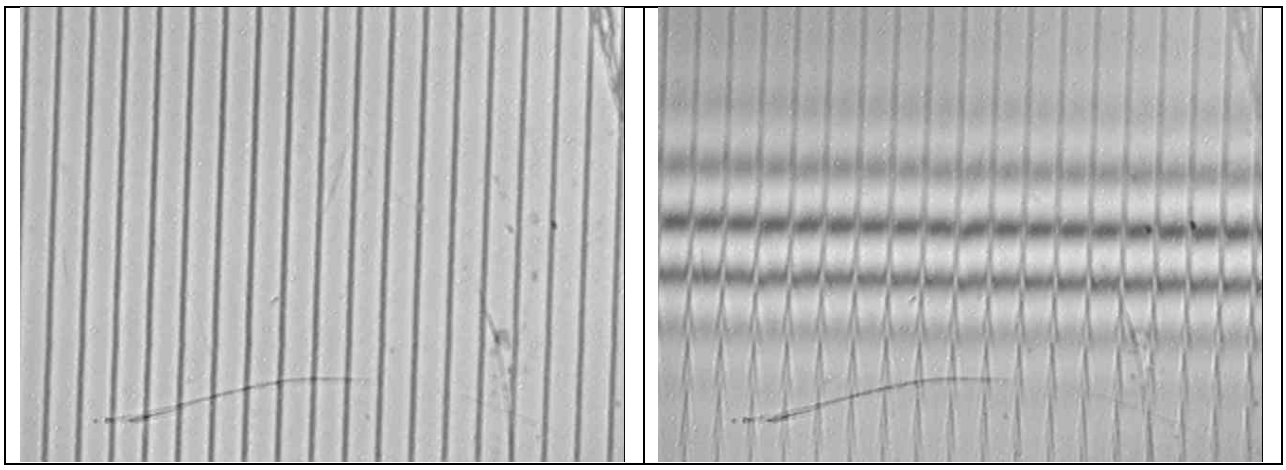

Fig. 2.35. shows a view of the microinterferometer's field of vision in the mode of interference using the object of the micrometer with a division value of 10 mcm as a sample.

2.6.2. Studies of inherent interference fringe patterns obtained from samples of transparencies with etching on glass and from samples with submicron pattern of 0.5–0.9 mcm.

In addition to the earlier mentioned experimental studies that lead to the following conclusions (see Report No. 1, [43]) the research work "Photomask" included a series of experimental studies that decisively confirmed the conclusions below.

Conclusions from Chapter 2.

1. Theoretical and experimental studies of matrix transparencies with four-level fractal ordered patterns lead to the conclusion that the resulting matrix topologies in the optical spectrum of 0.4….14 mcm can be interpreted as diffraction gratings with high quality of execution of reflecting (or shading) lines.
2. In IR range diffraction properties of those gratings can be partially explained by equations of wave optics because the primary structure of transparency patterns comes down to two mutually unfolded gratings: an orthogonal one (∂ =1.6 mcm; l?50 mcm) and a diagonal one (∂ =1.6 mcm; l=10$\sqrt{5}$ mcm). These transparencies in the IR range function as stop filters in transmission, and in reflection they produce an interference

fringe pattern with specific properties. In the visible light range of ECM, the matrices in question behave as secondary generators of a raster structure. In a laser flow in reflection, transparency matrices create a system of spatial rasters generated on four axes shifted from each other for $\frac{\pi}{4}$ rad.

In a laser flow in transmission, transparency matrices behaves as an analyzer of spatial frequencies. The laser flow patterns transmitted through the matrix directly from the source fully coincide with the spatial Fourier spectrum generated by means of a diffractometer.